Supporting Information for:

Single molecule observation of hard-soft-acid-base (HSAB) interaction in engineered *Mycobacterium smegmatis* porin A (MspA) nanopores

Sha Wang,[ab] Jiao Cao,[ab] Wendong Jia,[ab] Weiming Guo,[ab] Shuanghong Yan,[ab] Yuqin Wang ,[ab] Panke Zhang,[a] Hong-Yuan Chen*[a] and Shuo Huang*[ab]

[a] State Key Laboratory of Analytical Chemistry for Life Sciences, School of Chemistry and Chemical Engineering, Nanjing University, 210023, Nanjing, China

[b] Chemistry and Biomedicine Innovation Center (ChemBIC), Nanjing University, 210023, Nanjing, China

Corresponding Authors:

Prof. Hong-Yuan Chen: hychen@nju.edu.cn

Prof. Shuo Huang: shuo.huang@nju.edu.cn

Table of contents

Materials

Pentane, hexadecane, tris(2-carboxyethyl) phosphine hydrochloride (TCEP), ethylenediaminetetraacetic acid (EDTA) and Genapol X-80 were from Sigma-Aldrich. 1,2-diphytanoyl-sn-glycero-3-phosphocholine (DPhPC) was supplied by Avanti Polar Lipids. Sodium chloride (99.999%), calcium chloride anhydrous (99.99%), manganese sulfate monohydrate (99.99%), zinc sulfate heptahydrate (99.995%), cobalt sulfate heptahydrate (99.99%), nickel sulfate hexahydrate (99.99%), lead chloride (99.99%), cadmium sulfate, 8/3-hydrate (99.99%), sodium hydroxide (99.9%), sodium hydrogen phosphate and sodium dihydrogen phosphate were from Aladdin (China). 4-(2-hydroxyethyl)-1-piperazine ethanesulfonic acid (HEPES) was from Shanghai Yuanye Bio-Technology (China). Chelex 100 chelating resin (biotechnology grade, 100-200 mesh, sodium form), Precision Plus Protein™ Dual Color Standards and TGX™ FastCast™ Acrylamide Kit (12%) were from Bio-Rad.

Dioxane-free isopropyl-β-D-thiogalactopyranoside (IPTG), kanamycin sulfate and imidazole were from Solarbio Biotechnology (China). *E. coli* strain BL21 (DE3) were from Biomed. Luria-Bertani (LB) broth and LB agar were from Hopebio (China). Hydrochloric acid (HCl) was from Sinopharm (China). All the items listed aboved were used as received.

Methods

1. Preparation of mutant MspA proteins

To investigate single molecule coordination interactions between different combinations of amino acid residues and metal ions, the amino acid at the narrowest restriction (site 91) of an octameric MspA nanopore[1] was engineered. To achieve this, the gene coding for monomeric MspA-D (D93N/D90N/D118R/D134R/E139K), MspA-H (D93N/D91H/D90N/D118R/D134R/E139K) and MspA-C (D93N/D91C/D90N/D118R/D134R/E139K) were custom synthesized and constructed in a pet 30a(+) plasmid (Genscript, New Jersey) respectively. The D, H or C character in the

name of each gene stands for the aspartic acid, the histidine or the cysteine at site 91. A hexahistidine tag at the C-terminus of each gene was designed for purification purposes. The target proteins were expressed by *E. Coli* BL21 (DE3) and purified by nickel affinity chromatography as previously published.[2] Briefly, the constructed plasmid gene was heat-shock transformed into *E. Coli* BL21 (DE3). Afterwards, the cells were grown in LB medium to an OD_{600}=0.7, induced with 1 mM IPTG and shaken (180 rpm) overnight at 16 °C. The cells were harvested by centrifugation (4000 rpm, 20 min, 4 °C). The collected pellet was re-suspended in the lysis buffer (100 mM Na_2HPO_4/NaH_2PO_4, 0.1 mM EDTA, 150 mM NaCl, 0.5% (w/v) Genapol X-80, pH 6.5) and heated to 60 °C for 10 min. The suspension was cooled on ice for 10 min and centrifuged at 4 °C for 40 min at 13,000 rpm. After syringe filtration, the supernatant was loaded to a nickel affinity column (HisTrapTM HP, GE Healthcare). The column was first eluted with buffer A (0.5 M NaCl, 20 mM HEPES, 5 mM imidazole, 0.5% (w/v) Genapol X-80, pH=8.0) and further eluted with a linear gradient of imidazole (5 mM-500 mM) by mixing buffer A with buffer B (0.5 M NaCl, 20 mM HEPES, 500 mM imidazole, 0.5% (w/v) Genapol X-80, pH=8.0). The elution flow rate was set at 1 mL/min and the total elution volume was 30 mL. The eluted fractions were further characterized by SDS-polyacrylamide gel electrophoresis (PAGE) and the desired protein was identified. The identified fraction was immediately used for electrophysiology measurements or stored at -80 ℃ for long term storage. Characterizations of three MspA mutants were demonstrated in **Figures S1-S3** with more details.

The plasmid DNA containing the gene coding for MspA-D (Plasmid ID: 68731), MspA-H (Plasmid ID: 68732) and MspA-C nanopore (Plasmid ID: 68733) can be requested from the “Molecular Cloud” plasmid repository platform supported by Genscript (New Jersey, USA). Citation of this paper is requested.

2. Planar lipid bilayer recordings

As reported, a free standing, self-assembled lipid bilayer (DPhPC, Avanti Polar lipids,

USA) was formed between two 0.5 mL compartments filled with a measurement buffer (1 M NaCl, 10 mM HEPES at pH 7.40 ± 0.05).[3] To minimize contamination from other divalent metal ions, the measurement buffer was prepared with NaCl of the highest grade (99.999%, Aladdin, China). Prior to use, the measurement buffer was further mixed with Chelex 100 chelating resins (Bio-Rad), stirred for 4 h, pH adjusted and membrane filtered.

A pair of Ag/AgCl electrodes, which were electrically connected to a patch clamp amplifier (Axon 200B, Molecular Devices, USA), were placed in the electrolyte buffer in each compartment. Conventionally, the compartment which is electrically grounded is named the *cis* whereas the opposing compartment is named the *trans*. Single channel recording is performed when a single MspA nanopore (MspA-D, MspA-H or MspA-C) is inserted in the bilayer. Specifically for the measurement with MspA-C, tris(2-carboxyethyl) phosphine hydrochloride (TCEP) was added to the buffer with a 0.4 mM final concentration to prevent the formation of the disulfide bond within an octameric MspA-C.

All electrophysiology measurements were performed with a continuously applied +100 mV potential. The ionic current through a single nanopore was acquired with an Axopatch 200B patch clamp amplifier, sampled with a digitizer (Digidata 1550B) with a 25 kHz sampling rate and low-pass filtered with a 1 kHz corner frequency. All experiments were conducted at room temperature (21 ± 2 °C).

3. Data analysis

All channel binding events were detected by performing “single-channel search” using Clampfit 10.7 (Molecular Devices) and further analyzed (histogram generation, curve fitting and plotting) using OriginPro 8.5. The rate constants for the interaction between the amino acid residues and metal ions were derived from the equation: $k_{on}=1/(\tau_{on}[metal\ ions])$; $k_{off}=1/\tau_{off}$; $K_b=k_{on}/k_{off}$.

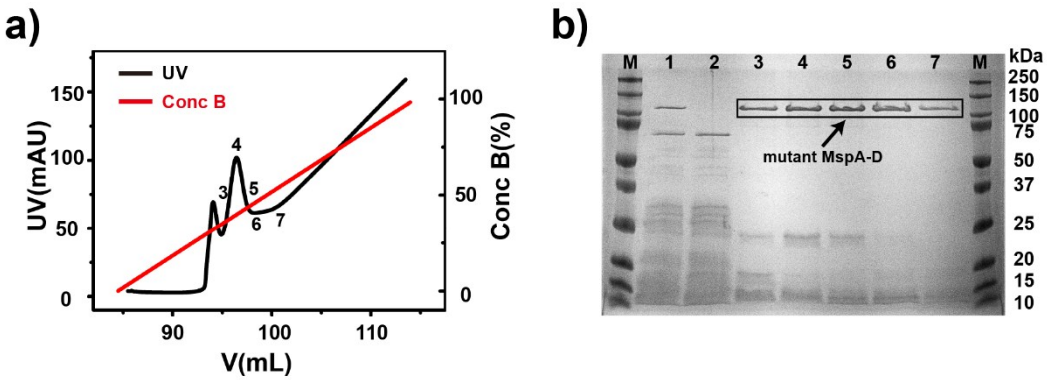

Figure S1. Purification and characterization of octameric MspA-D. a) The UV absorbance spectrum during column elution. The bacterial lysate from the prokaryotic expression of MspA-D **(Supplementary Methods 1)** was loaded on a nickel affinity column and eluted with a gradient of imidazole **(Supplementary Methods 1)**. The marked fractions were further characterized by gel electrophoresis. **b)** Gel electrophoresis of different elution fractions. The collected sample fractions were analyzed on a 12% homemade SDS-PAGE gel. Lanes: M, precision plus protein standards (BIO-RAD); 1, the supernatant of the bacteria lysate; 2, the eluted solution collected from the nickel affinity column immediately after bacteria lysate loading; 3-7, different sample fractions when the affinity column was further eluted with a gradient of imidazole, as demonstrated in **a)**. The band which lies between the molecular standard of 100 and 150 kDa, disappeared in lane 2 and appeared in lane 3-7. According to previously published results[2], this band results from the octameric MspA proteins. Fraction 7 was selected for subsequent nanopore measurements with no further purifications.

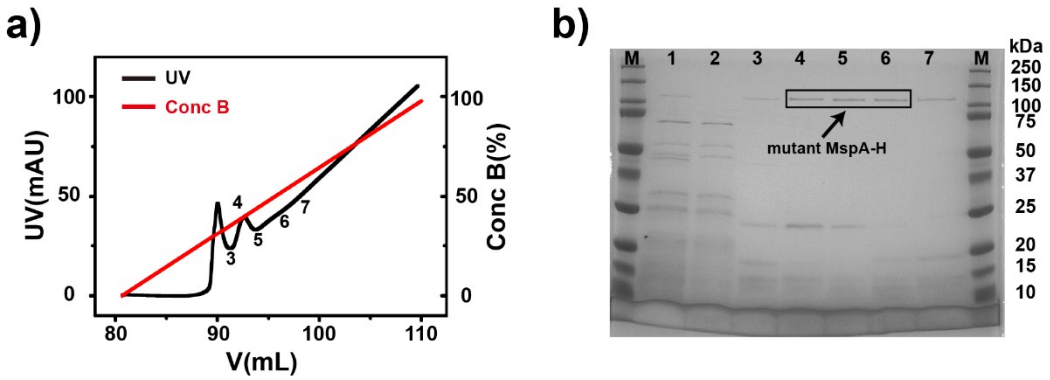

Figure S2. Purification and characterization of octameric MspA-H. a) The UV absorbance spectrum during column elution. The bacterial lysate from the prokaryotic expression of MspA-H **(Supplementary Methods 1)** was loaded on a nickel affinity column and eluted with a gradient of imidazole **(Supplementary Methods 1)**. The marked fractions were further characterized by gel electrophoresis. **b)** Gel electrophoresis of different elution fractions. The collected sample fractions were analyzed on a 12% homemade SDS-PAGE gel. Lanes: M, precision plus protein standards (BIO-RAD); 1, the supernatant of the bacteria lysate; 2, the eluted solution collected from the nickel affinity column immediately after bacteria lysate loading; 3-7, different sample fractions when the affinity column was further eluted with a gradient of imidazole, as demonstrated in **a)**. The band which lies between the molecular standard of 100 and 150 kDa, disappeared in lane 2 and appeared in lane 3-7. According to previously published results[2], this band results from the octameric MspA proteins. Fraction 6 was selected for subsequent nanopore measurements with no further purifications.

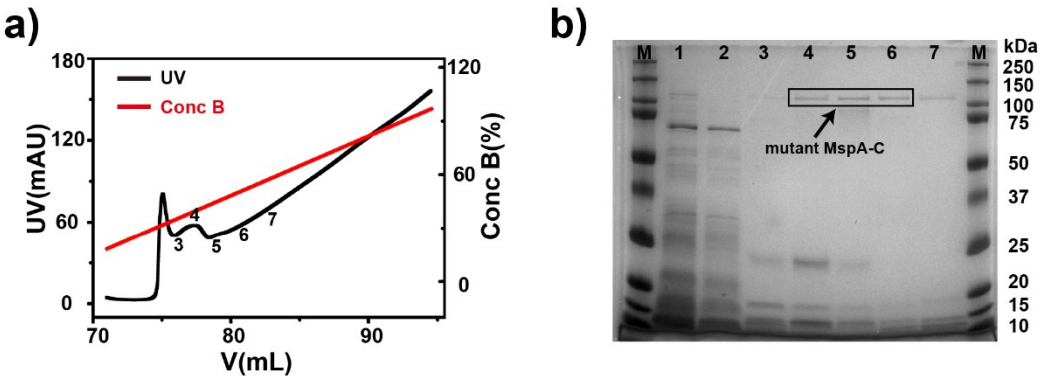

Figure S3. Purification and characterization of octameric MspA-C. a) The UV absorbance spectrum. The bacterial lysate from the prokaryotic expression of MspA-C **(Supplementary Methods 1)** was loaded on a nickel affinity column and eluted with a gradient of imidazole **(Supplementary Methods 1)**. The marked fractions were further characterized by gel electrophoresis. **b)** Gel electrophoresis of different elution fractions. The collected sample fractions were analyzed on a 12% homemade SDS-PAGE gel. Lanes: M, precision plus protein standards (BIO-RAD); 1, the supernatant of the bacteria lysate; 2, the eluted solution collected from the nickel affinity column immediately after bacteria lysate loading; 3-7, different sample fractions when the affinity column was further eluted with a gradient of imidazole, as demonstrated in **a)**. The band which lies between the molecular standard of 100 and 150 kDa, disappeared in lane 2 and appeared in lane 3-7. According to previously published results[2], this band results from the octameric MspA proteins. Fraction 6 was selected for subsequent nanopore measurements with no further purifications.

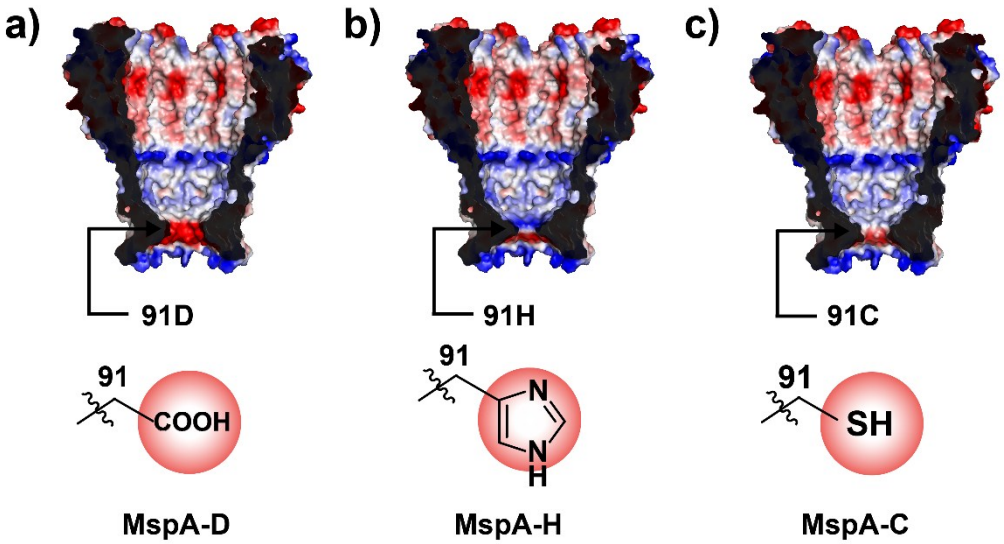

Figure S4: Charge distribution of three mutant MspA nanopores. Cross sectional views of octameric **a)** MspA-D, **b)** MspA-H and **c)** MspA-C nanopores (PDB ID: 1UUN). Protein nanopores are presented as surface representations and colored according to their "in vacuum" electrostatics (red for negative regions, and blue for positive regions). The demonstrated results were generated using Pymol.

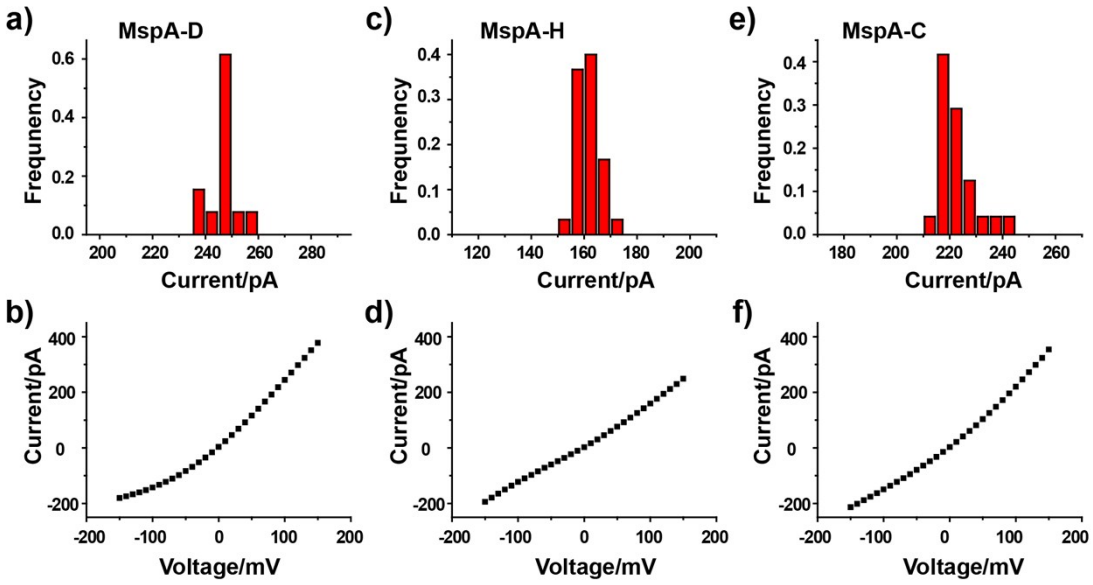

Figure S5. Statistics of open pore currents and I-V curves. The open pore current was measured with a buffer of 1 M NaCl, 10 mM HEPES, pH 7.4 and with a +100 mV continuously applied potential. All measurements were carried out at a temperature of 21 ± 2 °C. **a)** The open pore current histogram of MspA-D (N=13). **b)** I-V curve of a representative MspA-D nanopore. **c)** The open pore current histogram of MspA-H (N=30). **d)** I-V curve of a representative MspA-H nanopore. **e)** The open pore current histogram of MspA-C (N=24). **f)** I-V curve of a representative MspA-C nanopore. Specifically for MspA-C, a further addition of TCEP was performed with a final concentration of 0.4 mM to avoid the formation of a disulfide bond within the pore restriction. Though differs with only a single amino acid residue on site 91, the open pore conductance of all three MspA octamers appear to be different, following an order of MspA-D ~ MspA-C > MspA-H. This may be qualitatively explained as the imidazole group takes a larger space than the cysteine and the aspartic acid.[4] Besides, the aspartic acid residue on MspA-D and the cysteine residue on MspA-C, which is deprotonated or partially deprotonated during the measurement, enable the pore a cation selectivity,[5] which explains why a rectification effect from the I-V curve of MspA-D and MspA-C was observed but not from that of MspA-H.

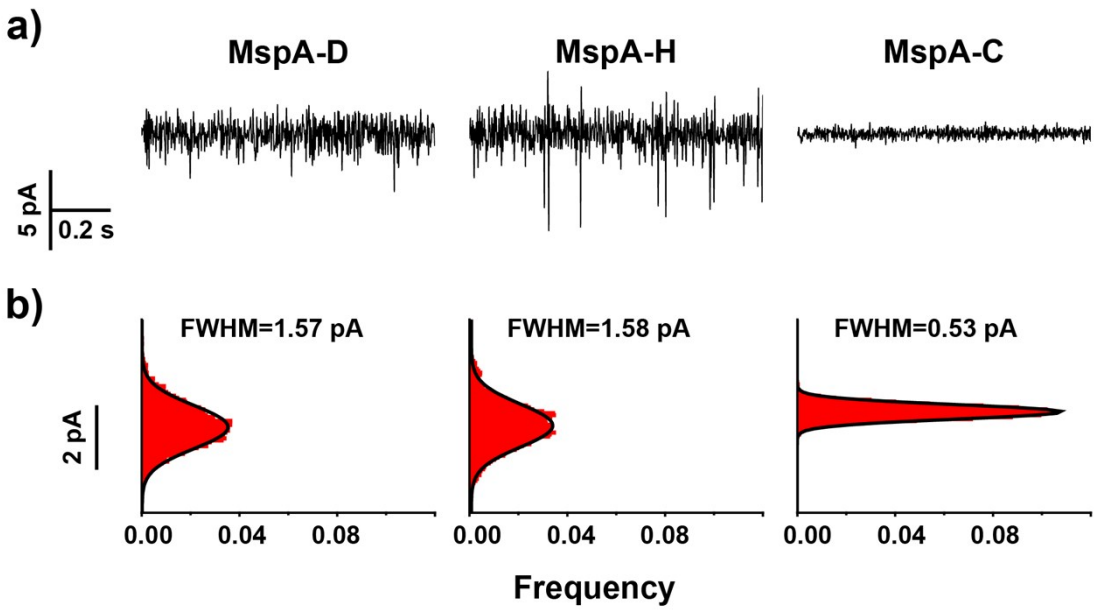

Figure S6. Background noise. Without the addition of any analyte, three octameric MspA mutants (MspA-D, H or C) demonstrate different background noises during single channel recordings. The measurements for MspA-D and MspA-H were performed with a buffer of 1 M NaCl, 10 mM HEPES, pH 7.4 and with a +100 mV continuously applied potential. Specifically for MspA-C, a further addition of TCEP was performed with a final concentration of 0.4 mM to avoid the formation of disulfide bonds within the pore restriction. For a fair comparison, all demonstrated results were acquired with an Axopatch 200B patch clamp amplifier, sampled with a digitizer (Digidata 1550B) with a 25 kHz sampling rate and low-pass filtered with a 1 kHz corner frequency. All experiments were conducted at room temperature (21 ± 2 °C). **a)** Background current traces acquired from different MspA mutants. **b)** The corresponding all-points histogram of **a)**. The histograms were Gaussian fitted. From the full width of half maximum (FWHM), it is clearly demonstrated that the MspA-D and the MspA-H mutant generate excessive current noise compared with that of MspA-C. The FWHM measures 1.47 ± 0.11 pA for MspA-D, 1.52 ± 0.055 pA for MspA-H and 0.52 ± 0.046 pA for MspA-C. The mean and standard deviation values of FWHM were based on three independent experiments for each pore (N=3).

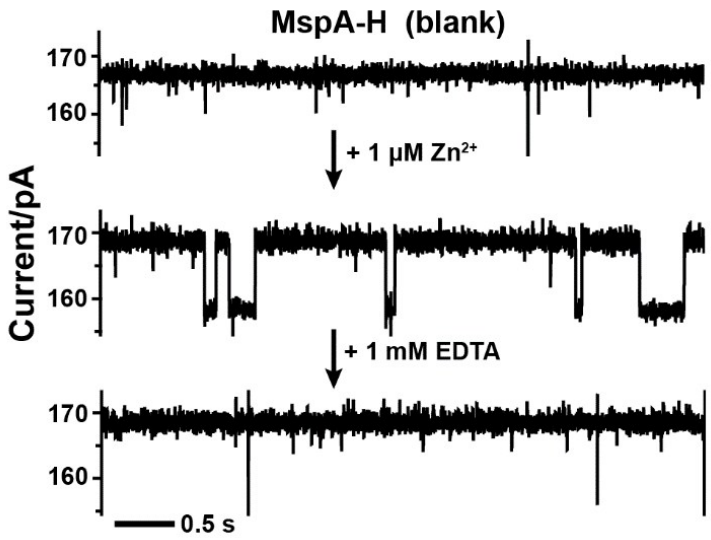

Figure S7. Verification of Zn^{2+} binding events. During single channel recordings with MspA-H, stochastic pore blockage events appeared immediately after the addition of Zn^{2+} to the *trans* compartment with a 1 μM final concentration. With a further addition of EDTA, which is a chelating agent of Zn^{2+}, to the *trans* with a 1 mM final concentration, the pore blockage signals immediately disappeared. This experiment further verifies that the observed pore blockage events results from the coordination of Zn^{2+} to the pore restriction. The demonstrated single-channel recordings were performed with a buffer of 1 M NaCl, 10 mM HEPES, pH 7.4 in both compartments and a +100 mV potential was continously applied.

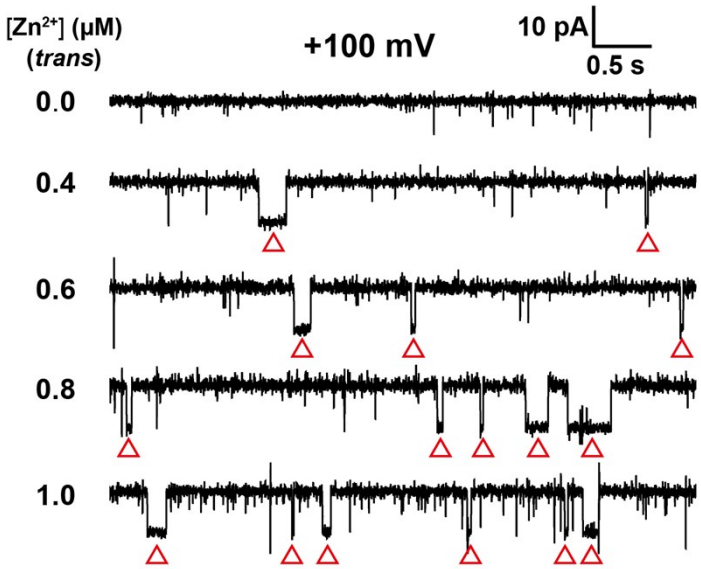

Figure S8. Reversible binding of Zn^{2+} to MspA-H. During single channel recordings with MspA-H, the rate of event appearance was increased when the concentration of Zn^{2+} in the *trans* was increased from 0, 0.6, 0.8 to 1.0 μM. Red triangles mark signals generated from Zn^{2+} binding to the pore. The demonstrated single channel recordings were performed with a buffer of 1 M NaCl, 10 mM HEPES, pH 7.4 in both compartments and a +100 mV potential was continously applied.

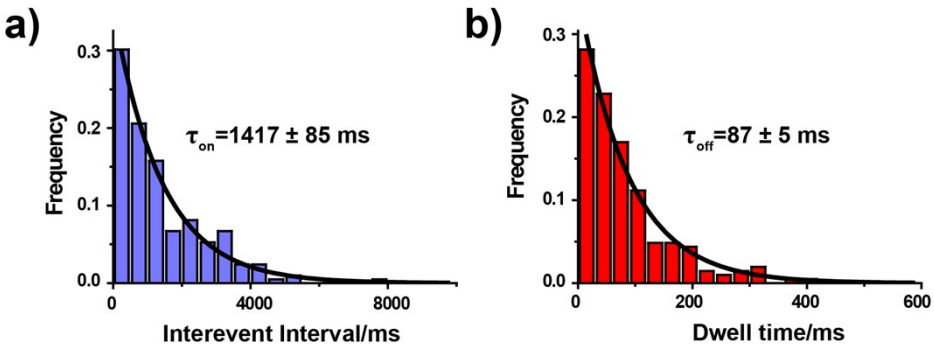

Figure S9. τ_{on} **and** τ_{off} **of Zn^{2+} binding to MspA-H. a)** The mean interevent interval (τ_{on}) and **b)** the dwell time (τ_{off}) for events generated from the measurement with MspA-H. Zn^{2+} was added to the *trans* with a 1 µM final concentration. The demonstrated single channel recordings were performed with a buffer of 1 M NaCl, 10 mM HEPES, pH 7.4 in both compartments and a +100 mV potential was continously applied.

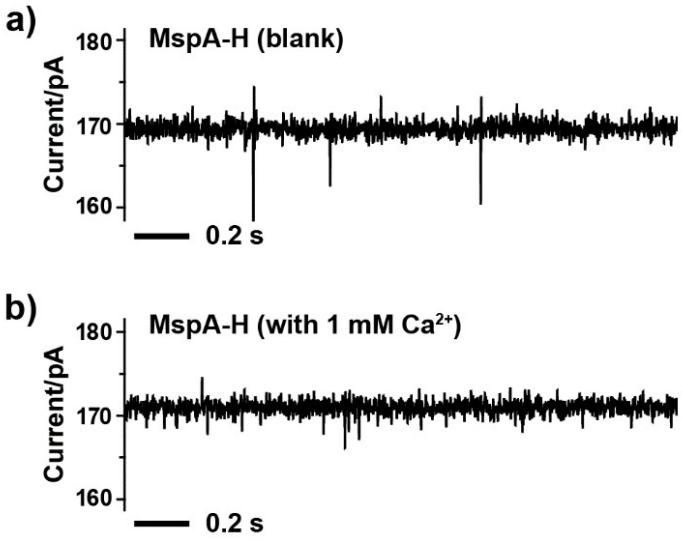

Figure S10. MspA-H with Ca^{2+}. Single channel recording of MspA-H before **a)** and after **b)** the addition of Ca^{2+} in the *trans* compartment reaching a 1 mM final concentration. No binding events were observed from Ca^{2+}. The demonstrated single channel recordings were performed with a buffer of 1 M NaCl, 10 mM HEPES, pH 7.4 in both compartments and a +100 mV potential was applied.

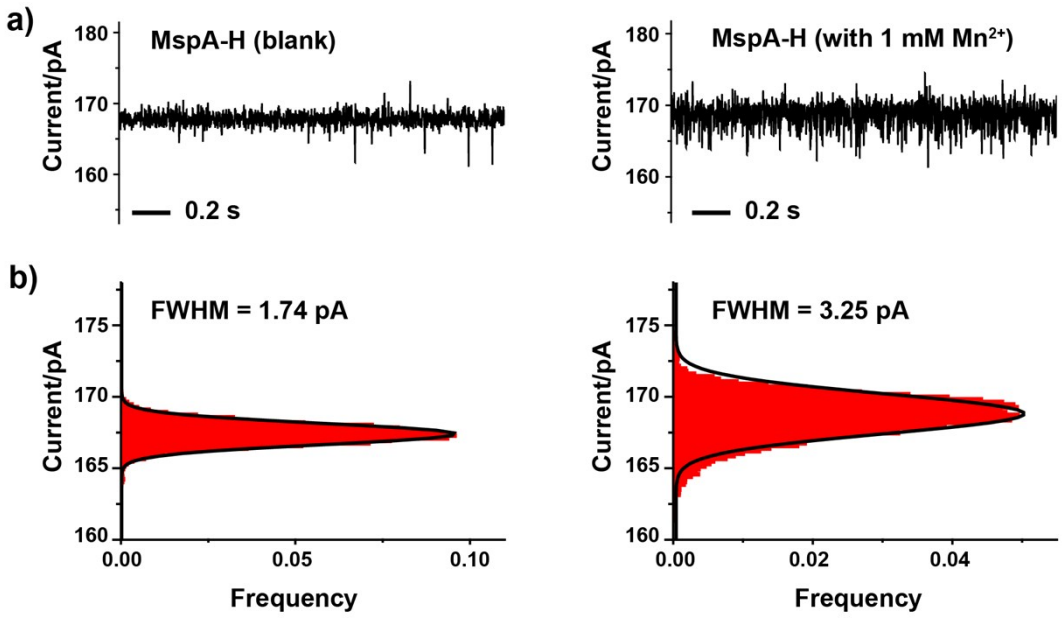

Figure S11. Interaction of MspA-H with Mn^{2+}. a). Single channel recording of MspA-H before and after the addition of Mn^{2+} in the *trans* compartment reaching a 1 mM final concentration. **b)** The corresponding all-points histogram of **a).** An apparent increase of the background noise was observed with the addition of Mn^{2+} with a 1 mM final concentration in *trans.* This indicates that weak interactions between Mn^{2+} and the histidine residue contibute to this noise. However, no discrete level of binding events from single Mn^{2+} ions was resolved. The mean FWHM for MspA-H measures 1.47 ± 0.11 pA and 3.19 ± 0.12 pA respectively before and after the addition of Mn^{2+} in the *trans* with a 1 mM final concentration. The measurements were performed with a buffer of 1 M NaCl, 10 mM HEPES, pH 7.4 in both compartments and with a +100 mV applied potential. Three independent measurements (N=3) were performed for each condition.

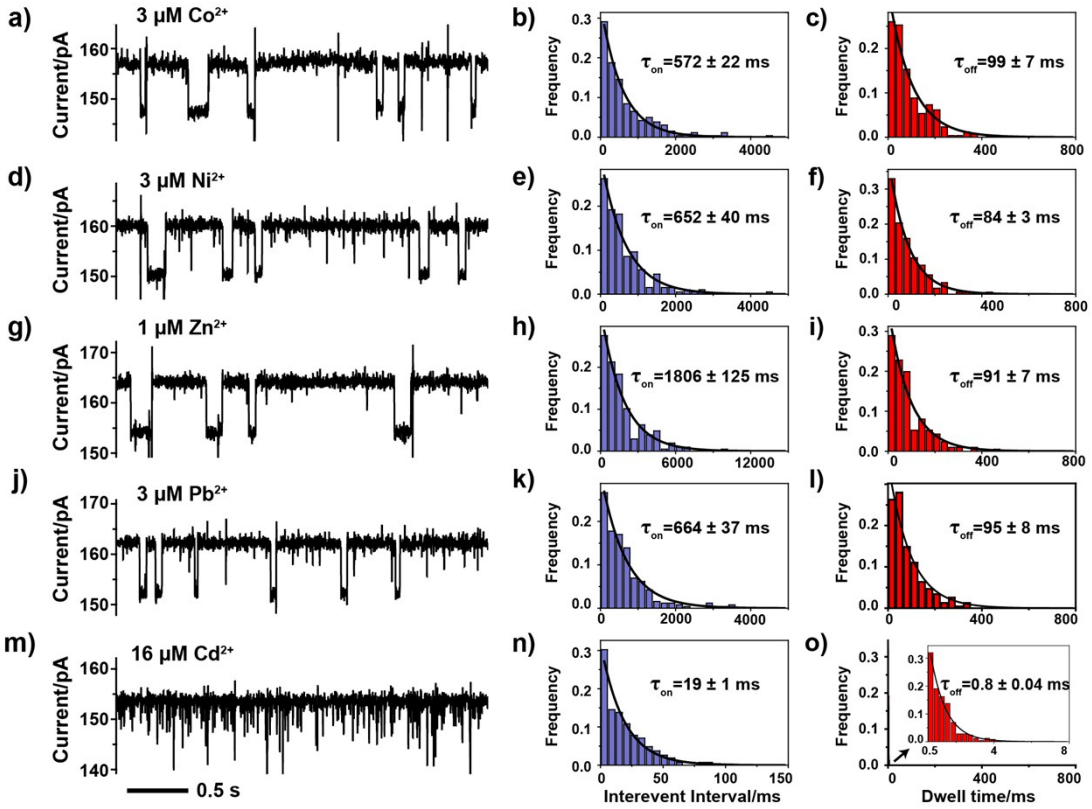

Figure S12. Interaction of MspA-H with metal ions. Binding events acquired from the MspA-H nanopore interacting with different metal ions. Corresponding statistics of the interevent intervals (τ_{on}) and the dwell times (τ_{off}) were also demonstrated. All data were acquired in a buffer of 1 M NaCl ,10 mM HEPES, pH 7.4 with a +100 mV applied potential. Solid lines are single exponential fitting to the histograms. Results from measuremnts with **a-c)** 3 μM Co^{2+}, **d-f)** 3 μM Ni^{2+}, **g-i)** 1 μM Zn^{2+}, **j-l)** 3 μM Pb^{2+} or **m-o)** 16 μM Cd^{2+} in the *trans* compartment are demonstrated respectively.

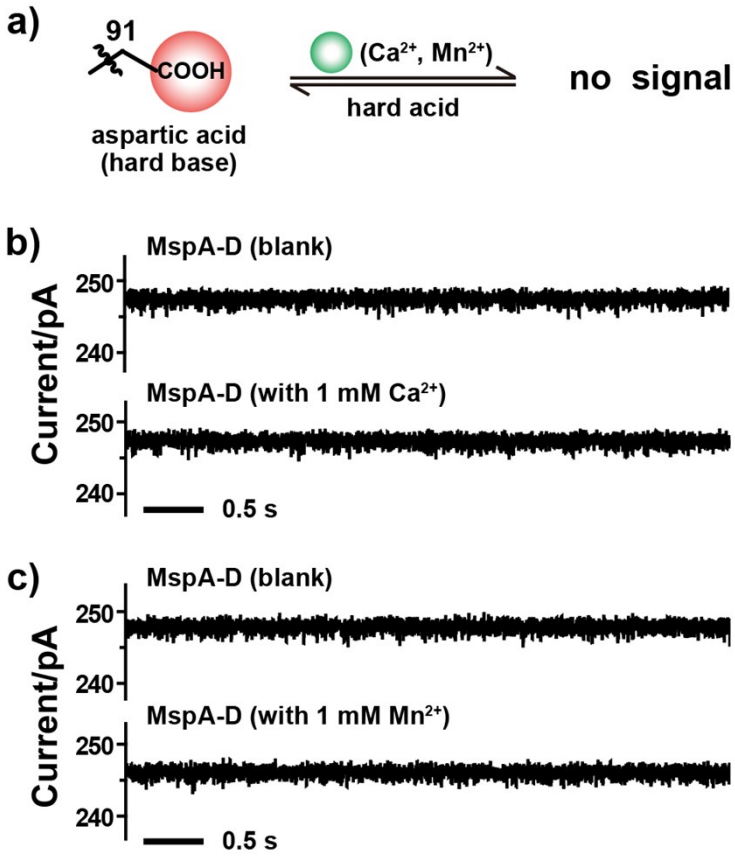

Figure S13. MspA-D with hard ions. a) Schematic diagram of the coordination interaction between an aspartic acid residue (hard base) within the MspA-D nanopore and hard acid ions (Ca^{2+} or Mn^{2+}). **b)** Single channel recording of MspA-D before and after the addition of Ca^{2+} in the *trans* compartment reaching a 1 mM final concentration. **c)** Single channel recording of MspA-D before and after the addition of Mn^{2+} in the *trans* compartment reaching a 1 mM final concentration. No binding events from Ca^{2+} or Mn^{2+} were detected, as demonstrated in **b)** and **c)**. The demonstrated single-channel recordings were performed with a buffer of 1 M NaCl, 10 mM HEPES (pH 7.4) in both compartments and a +100 mV potential was continously applied.

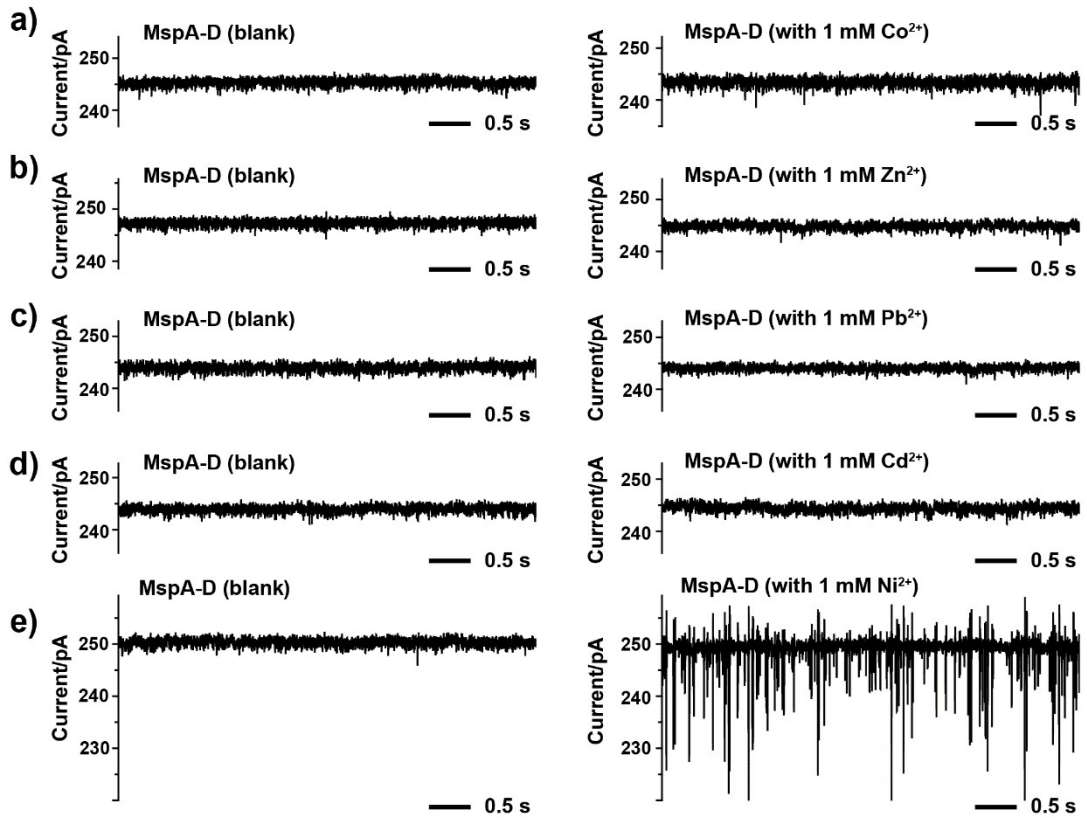

Figure S14. MspA-D with other metal ions. a), b), c), d) Single channel recordings of MspA-D before and after the addition of metal ions (Co^{2+}, Zn^{2+}, Pb^{2+}, Cd^{2+}) in the *trans* compartment reaching a 1 mM final concentration respectively. No binding events from these metal ions were detected. **e)** Single channel recording of MspA-D before and after the addition of Ni^{2+} in the *trans* compartment reaching a 1 mM final concentration. Spiky signals with a wide dispersion in the blockage depth were observed. The demonstrated single-channel recordings were performed with a buffer of 1 M NaCl, 10 mM HEPES (pH 7.4) in both compartments and a +100 mV potential was continously applied.

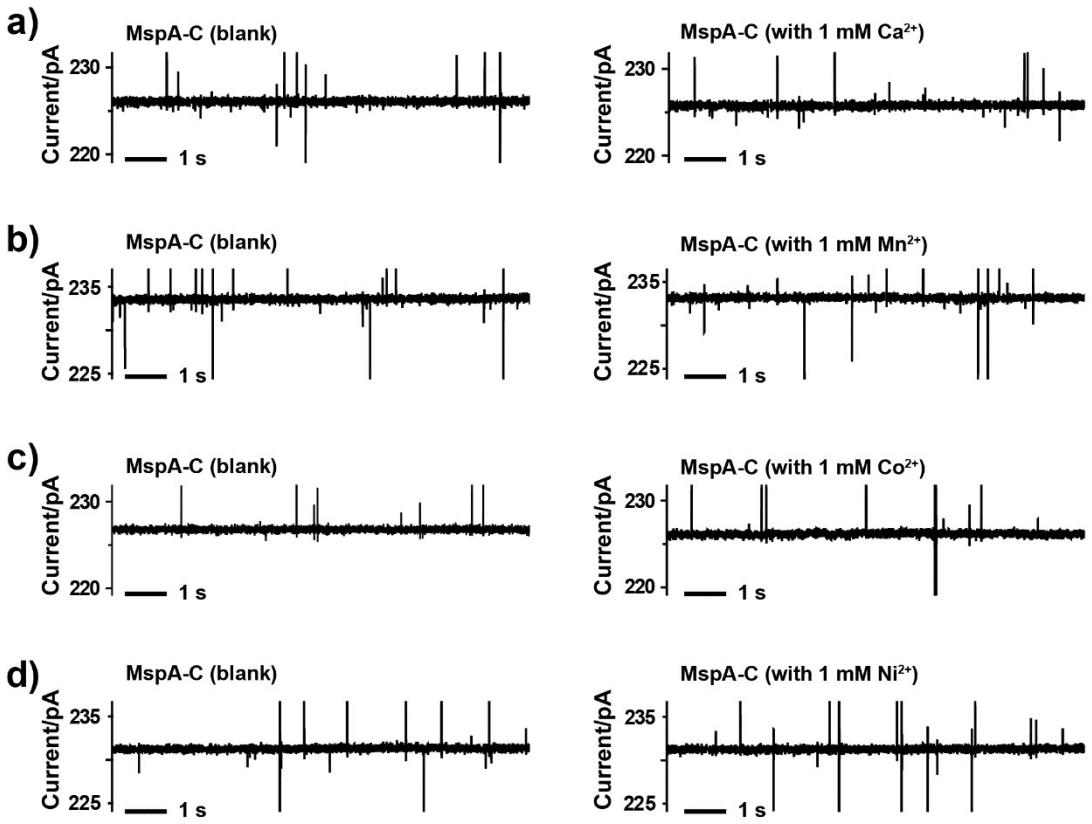

Figure S15. Interaction of MspA-C with metal ions. a-d) Single channel recordings of MspA-C before and after the addition of metal ions (Ca^{2+}, Mn^{2+}, Co^{2+}, Ni^{2+}) reaching a 1 mM final concentration in the *trans* compartment. None of these ions gave detectable signals when probed with MspA-C. All measurements were performed with a buffer of 1 M NaCl, 10 mM HEPES, 0.4 mM TCEP, pH 7.4 in both compartments and with a +100 mV applied potential. Spiky background noises that appear before the addition of any analytes originate from MspA-C itself.

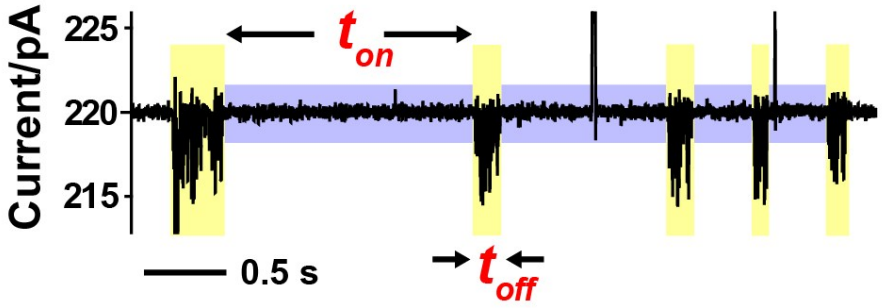

Figure S16. Pb^{2+} binding with MspA-C. During single channel recording, Pb^{2+} interacts with the sulfhydryl group around the restriction of an MspA-C nanopore, which resulted in binding events in the shape of clusters (marked yellow). Each cluster was treated as a single binding event. The dwell time (t_{off}) and the inter-event interval (t_{on}) is defined as depicted in the Figure. The measurement was performed with a buffer of 1 M NaCl, 10 mM HEPES, 0.4 mM TCEP in both compartments and a +100 mV potential was applied.

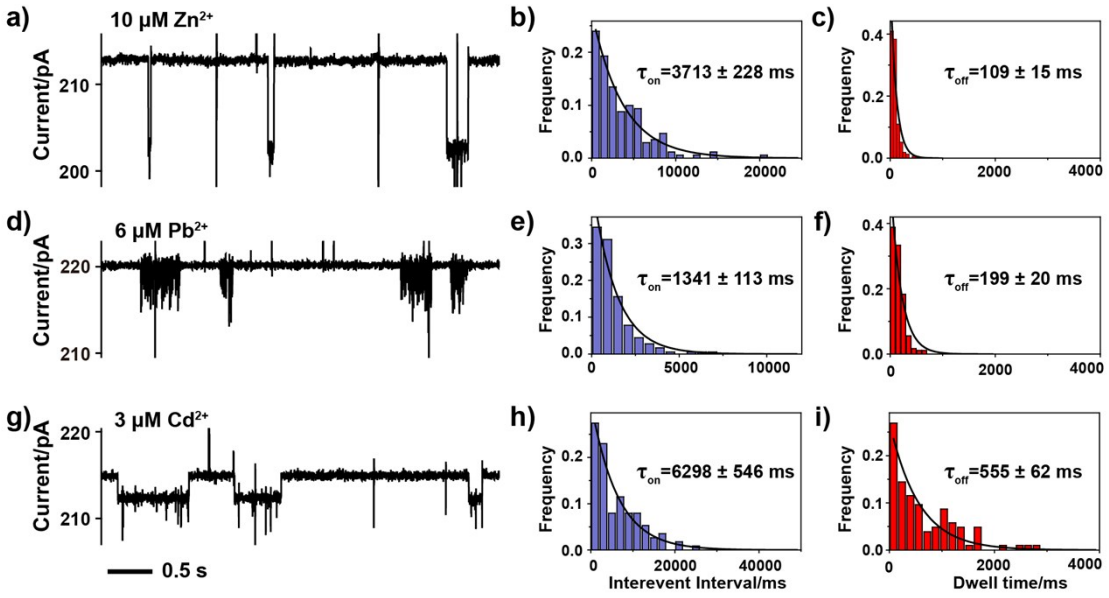

Figure S17. Interaction of MspA-C with other metal ions. a), b), c), The demonstration of single metal ion binding events acquired from the MspA-C nanopore and the statistics of the interevent intervals (τ_{on}) and the dwell times (τ_{off}). All data were acquired with the buffer of 1 M NaCl ,10 mM HEPES, 0.4 mM TCEP, pH 7.4 with a +100 mV applied potential. Solid lines are single exponential fitting to the histograms. Results from measurements with **a-c)** 10 μM Zn^{2+}, **d-f)** 6 μM Pb^{2+}, **g-i)** 3 μM Cd^{2+} in the *trans* compartment are demonstrated.

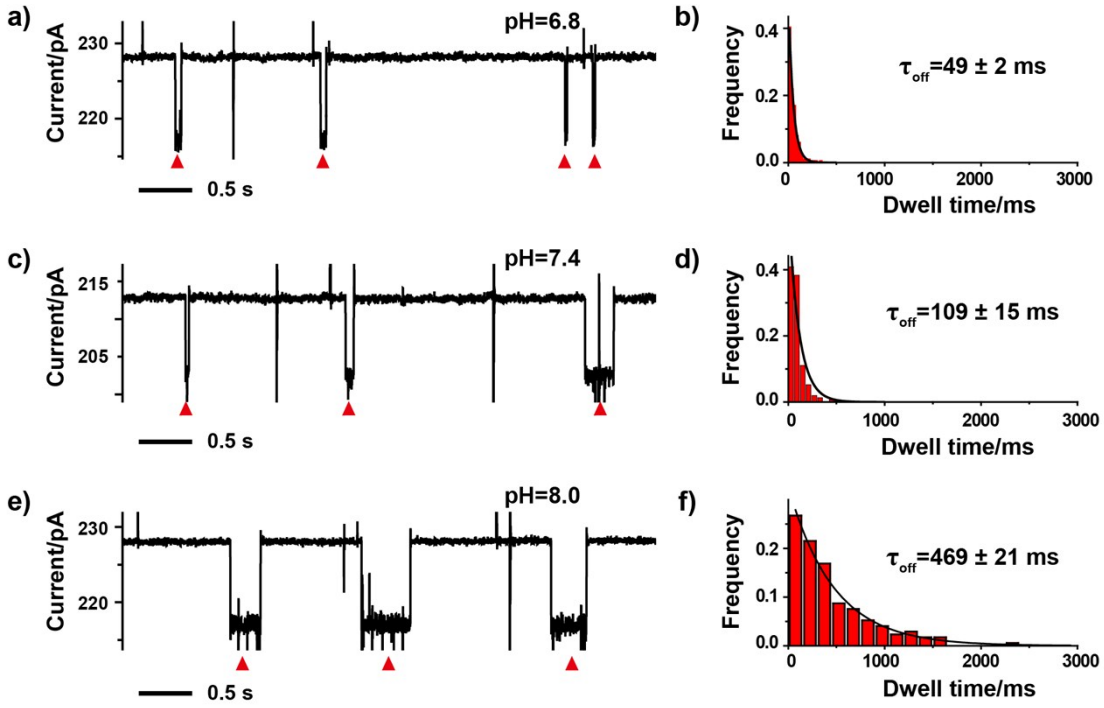

Figure S18. Zn^{2+} binding to MspA-C at different pH. Single channel recordings were performed with a buffer of 1 M NaCl, 10 mM HEPES, 0.4 mM TCEP in both compartments and with a +100 mV applied potential. **a-b)** The measurement buffer was pH adjusted to 6.8. Zn^{2+} was added to the *trans* with a 30 μM final concentration. **a)** A representative current trace acquired with this condition. **b)** The corresponding histogram of the event dwell time. **c-d)** The measurement buffer was pH adjusted to 7.4. Zn^{2+} was added to the *trans* with a 10 μM final concentration. **c)** A representative current trace acquired with this condition. **d)** The corresponding histogram of the event dwell time. **e-f)** The measurement buffer was pH adjusted to 8.0. Zn^{2+} was added to the *trans* with a 8 μM final concentration. **e)** A representative current trace acquired with this condition. **f)** The corresponding histogram of the event dwell time. The dwell time of Zn^{2+} binding events systematically extends when the measurement was performed with a buffer of a higher pH. Red triangles mark the Zn^{2+} binding events.

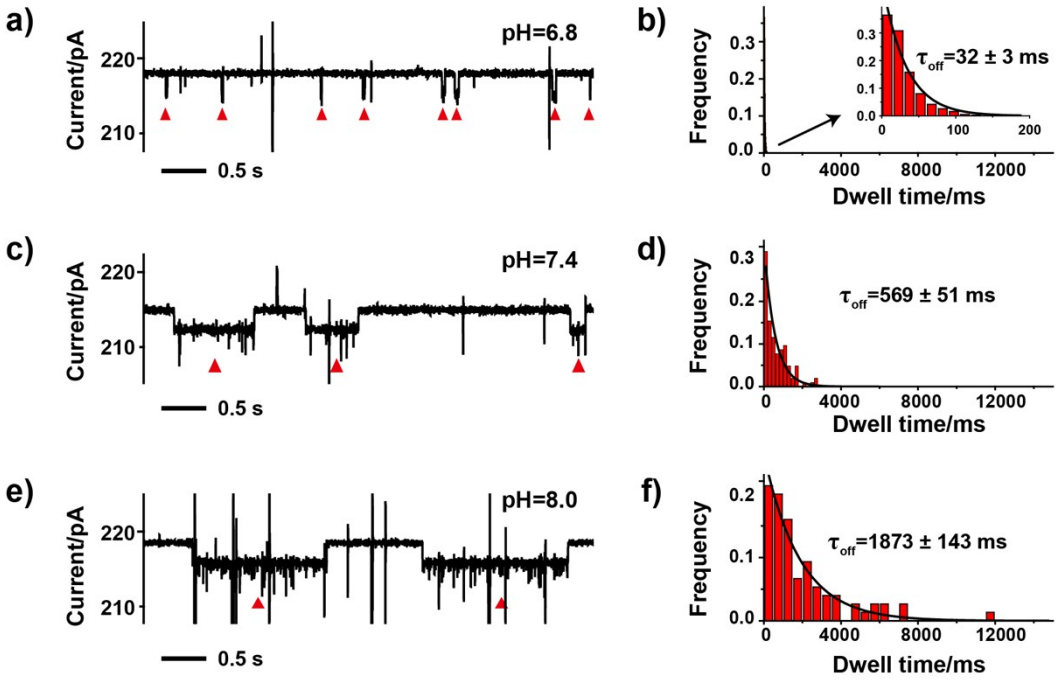

Figure S19. Cd^{2+} binding to MspA-C at different pH. Single channel recordings were performed with a buffer of 1 M NaCl, 10 mM HEPES, 0.4 mM TCEP in both compartments and with a +100 mV applied potential. **a-b)** The measurement buffer was pH adjusted to 6.8. Cd^{2+} was added to the *trans* with a 20 μM final concentration. **a)** A representative current trace acquired with this condition. **b)** The corresponding histogram of the event dwell time. **c-d)** The pH of the measurement buffer was adjusted to 7.4. Cd^{2+} was added to the *trans* with a 4 μM final concentration. **c)** A representative current trace acquired with this condition. **d)** The corresponding histogram of the event dwell time. **e-f)** The pH of the measurement buffer was adjusted to 8.0. Cd^{2+} was added to the *trans* with a 4 μM final concentration. **e)** A representative current trace acquired with this condition. **f)** The corresponding histogram of the event dwell time. The dwell time of Cd^{2+} binding events systematically extends when the measurement was performed with a buffer of a higher pH. Red triangles mark the Cd^{2+} binding events.

Table S1: Open pore currents of three mutant MspA nanopores.

Nanopore Protein	Pores Numbers (N)	Open Pore Current (pA)
MspA-D[a]	N=13	245.7 ± 5.8
MspA-H[a]	N=30	161.1 ± 4.0
MspA-C[b]	N=24	222.0 ± 6.8

[a] Condition: 1 M NaCl, 10 mM HEPES, pH 7.4, at +100 mV, 21 ± 2 °C.

[b] Condition: 1 M NaCl, 10 mM HEPES, 0.4 mM TCEP, pH 7.4, at +100 mV, 21 ± 2 °C.

Table S2: Kinetic constants acquired between histidine (MspA-H) and metal ions[a].

metal ions	Current blockade(ΔI) (pA)	k_{on} ($M^{-1}s^{-1}$)	k_{off} (s^{-1})	K_b (M^{-1})[b]
Co^{2+}	9.5 ± 0.3	(6.8 ± 1.2)*10^5	10.5 ± 0.7	(6.5 ± 0.8)10*4
Ni^{2+}	9.9 ± 0.1	(5.7 ± 0.6)*10^5	11.8 ± 0.2	(4.9 ± 0.4)*10^4
Zn^{2+}	10.4 ± 0.5	(6.9 ± 1.1)*10^5	11.9 ± 1.5	(5.8 ± 0.4)*10^4
Pb^{2+}	9.8 ± 0.05	(5.3 ± 0.4)*10^5	10.4 ± 1.2	(5.1 ± 0.9)*10^4
Cd^{2+}	7.4 ± 0.4	(3.4 ± 0.4)*10^6	1452.9 ± 241.4	(2.3 ± 0.1)*10^3

[a] Condition: 1 M NaCl, 10 mM HEPES, pH 7.4, +100 mV.

[b] Binding constants (K_b) were derived according to the equation $K_b = k_{on}/k_{off}$.

Table S3: Kinetic constants acquired between cysteine (MspA-C) and metal ions[a].

metal ions	Current blockade(ΔI) (pA)	k_{on} ($M^{-1}s^{-1}$)	k_{off} (s^{-1})	K_b (M^{-1})[b]
Zn^{2+}	10.5 ± 0.2	(2.5 ± 0.2)*10^4	7.6 ± 1.1	(3.4 ± 0.6)*10^3
Pb^{2+}	—	(9.5 ± 1.8)*10^4	4.7 ± 0.2	(2.0 ± 0.5)*10^4
Cd^{2+}	2.7 ± 0.02	(6.2 ± 1.1)*10^4	2.3 ± 0.7	(2.8 ± 0.8)*10^4

[a] Condition: 1 M NaCl, 10 mM HEPES, 0.4 mM TCEP, pH 7.4, +100 mV.

[b] Binding constants (K_b) were derived according to the equation $K_b = k_{on}/k_{off}$.

Table S4: Zn^{2+} binding to MspA-C at different pH [a].

pH	Current blockade(ΔI) (pA)	k_{on} ($M^{-1}s^{-1}$)	k_{off} (s^{-1})	K_b (M^{-1})[b]
6.8	10.9 ± 0.4	(2.5 ± 0.8)*10^4	25.3 ± 3.8	(9.7 ± 1.9)*10^2
7.4	10.5 ± 0.2	(2.5 ± 0.2)*10^4	7.6 ± 1.1	(3.4 ± 0.6)*10^3
8.0	11.4 ± 0.1	(2.5 ± 1.0)*10^4	2.5 ± 0.4	(1.0 ± 0.1)*10^4

[a] Condition: 1 M NaCl, 10 mM HEPES, 0.4 mM TCEP, +100 mV.

[b] Binding constants (K_b) were derived according to the equation $K_b = k_{on}/k_{off}$.

Table S5: Cd^{2+} binding to MspA-C at different pH [a].

pH	Current blockade(ΔI) (pA)	k_{on} ($M^{-1}s^{-1}$)	k_{off} (s^{-1})	K_b (M^{-1})[b]
6.8	2.9 ± 0.2	(4.0 ± 1.2)*10^4	28.7 ± 10.4	(1.6 ± 1.1)*10^3
7.4	2.7 ± 0.02	(6.2 ± 1.1)*10^4	2.3 ± 0.7	(2.8 ± 0.8)*10^4
8.0	2.8 ± 0.06	(8.8 ± 1.8)*10^4	0.6 ± 0.2	(1.5 ± 0.3)*10^5

[a] Conditions: 1 M NaCl, 10 mM HEPES, 0.4 mM TCEP, +100 mV.

[b] Binding constants (K_b) were derived according to the equation $K_b = k_{on}/k_{off}$.

Video S1: Pb^{2+} binding to MspA-H. The demonstrated single channel recording was performed with a buffer of 1 M NaCl, 10 mM HEPES, pH=7.4 in both compartments. With a single MspA-H inserted in the membrane, Pb^{2+} was added to trans with a 3 μM final concentration and a +100 mV potential was continuously applied. Clearly resolvable resistive pulses in the video results from stochastic binding of Pb^{2+} to a histidine residue placed around the pore restriction of MspA-H, as demonstrated in **Figure S12j**.

Video S2: Pb^{2+} binding to MspA-C. The demonstrated single channel recording was performed with a buffer of 1 M NaCl, 10 mM HEPES, 0.4 mM TCEP, pH=7.4 in both compartments. With a single MspA-C inserted in the membrane, Pb^{2+} was added to trans

with a 6 μM final concentration and a +100 mV potential was continuously applied. Pb^{2+} binding to MspA-C results in cluster shaped events, which is different from any other single molecule binding events reported in this work. The cluster event results from stochastic binding of Pb^{2+} to a cysteine residue placed around the pore restriction of MspA-C, as demonstrated in **Figure S17d**.

Video S3: Zn^{2+} binding to MspA-C at pH 6.8. The demonstrated single channel recording was performed with a buffer of 1 M NaCl, 10 mM HEPES, 0.4 mM TCEP, pH=6.8 in both compartments. With a single MspA-C inserted in the membrane, Zn^{2+} was added to trans with a 30 μM final concentration and a +100 mV potential was continuously applied. At a lower pH (6.8), the observed Zn^{2+} binding events appear short in the dwell time (40 ± 7 ms), as demonstrated in **Figure S18a**.

Video S4: Zn^{2+} binding to MspA-C at pH 8.0. The demonstrated single channel recording was performed with a buffer of 1 M NaCl, 10 mM HEPES, 0.4 mM TCEP, pH=8.0 in both compartments. With a single MspA-C inserted in the membrane, Zn^{2+} was added to trans with a 30 μM final concentration and a +100 mV potential was continuously applied. At a higher pH (8.0), the observed Zn^{2+} binding events appear long in the dwell time (408 ± 69 ms), as demonstrated in **Figure S18e**.

Reference

1. T. Z. Butler, M. Pavlenok, I. M. Derrington, M. Niederweis and J. H. Gundlach, *Proc. Natl. Acad. Sci.* , 2008, **105**, 20647-20652.
2. Y. Wang, S. Yan, P. Zhang, Z. Zeng, D. Zhao, J. Wang, H. Chen and S. Huang, *ACS Appl. Mater. Interfaces*, 2018, **10**, 7788-7797.
3. S. Yan, X. Li, P. Zhang, Y. Wang, H.-Y. Chen, S. Huang and H. Yu, *Chem. Sci.*, 2019, **10**, 3110-3117.
4. G. Di Muccio, A. E. Rossini, D. Di Marino, G. Zollo and M. Chinappi, *Sci. Rep.*, 2019, **9**, 6440.
5. C. Wei, A. J. Bard and S. W. Feldberg, *Anal. Chem.*, 1997, **69**, 4627-4633.